Cell-Free Massive MIMO with Low-Resolution ADCs and I/Q Imbalance Over Spatially Correlated Channels

Zhilong Liu, Jiayi Zhang, Zhe Wang, Bo Ai, *Fellow, IEEE*, and Derrick Wing Kwan Ng, *Fellow, IEEE*

Abstract—In this paper, we investigate a cell-free massive multiple-input multiple-output (CF mMIMO) system with both multi-antenna user equipments (UEs) and access points (APs) over spatially correlated Rayleigh fading channels. In practical CF mMIMO systems, the in-phase and quadrature-phase imbalance (IQI) and low-resolution analog-to-digital converters (ADCs) at the APs are critical for the system performance. Taking these factors into account, the achievable uplink spectral efficiency (SE) is analyzed based on a two-layer decoding scheme. In particular, the maximum ratio (MR) and local minimum mean-square error (L-MMSE) combining are adopted at the APs while the large-scale fading decoding (LSFD) is implemented at the central processing unit (CPU). Furthermore, we derive novel closed-form SE expressions with the MR combining and investigate the SE performance for different combining schemes, quantization bits, and IQI parameters. Numerical results reveal the performance degradations caused by both the low-resolution ADCs and IQI. Additionally, increasing the number of APs is an effective means to promote the system performance.

I. Introduction

Cell-free massive multiple-input multiple-output (CF mMIMO), which is regarded as one of the most promising candidate technologies of the sixth-generation (6G), can significantly improve both the spectral efficiency (SE) and energy efficiency (EE) [1]–[4], due to its outstanding advantages of fully exploiting the spatial degrees-of-freedom. The unique feature of CF mMIMO systems is to deploy plenty of antennas at access points (APs) over a wide service area to serve fewer distributed user equipments (UEs) to effectively shorten the distances between the wireless transceivers [5].

Recently, various studies have been conducted in the literatures to unleash the potential of CF mMIMO. For example, the authors of [6] investigated four different uplink (UL) processing schemes from fully centralized implementation to fully distributed implementation, showing that the CF mMIMO system can achieve excellent performance with the minimum mean-square error (MMSE) processing schemes. Based on [6], the UL performance of CF mMIMO systems

Z. Liu, J. Zhang, and Z. Wang are with the School of Electronics and Information Engineering, Beijing Jiaotong University, Beijing 100044, P. R. China. (e-mail: jiayizhang@bjtu.edu.cn).

B. Ai is with the State Key Laboratory of Rail Traffic Control and Safety, Beijing Jiaotong University, Beijing 100044, China.

D. W. K. Ng is with the School of Electrical Engineering and Telecommunications, University of New South Wales, NSW 2052, Australia. (e-mail: w.k.ng@unsw.edu.au).

with multi-antenna UEs over Rayleigh fading channels was further analyzed in [4].

On the other hand, a massive number of radio-frequency (RF) chains should be deployed at APs, which would undoubtedly bring considerable data processing burden, high hardware costs, and high system power consumption. As a remedy, employing low-precision components in the devices of CF mMIMO systems is an effective technique to address the above problems [7]. For instance, the low-resolution analog-to-digital converters (ADCs) have been widely studied in CF mMIMO systems. By means of the additive quantization noise model (AQNM), the authors of [8] investigated the UL performance with low-resolution ADCs and showed that CF mMIMO outperforms conventional cellular massive MIMO and small-cell networks. Also, in [9], the UL SE and EE expressions were derived with the consideration of the low-resolution ADCs employed at the APs. It was found that a small bit resolution ADC in a CF mMIMO system is sufficient to achieve the same SE performance as the one with ideal ADCs. Furthermore, a mixed-ADC architecture deploying at the APs can facilitate the tradeoff exploration between the SE and EE over Rician fading channels [10].

Despite their potential benefits, the hardware impairments caused by low-quality components would also have a significant impact on the performance in practical CF mMIMO systems. For example, the in-phase and quadrature-phase imbalance (IQI) is a classical kind of hardware impairments. The author considered the impact of IQI on the achievable information rate with the MR combining and zero-forcing receivers in [11]. Besides, the MMSE estimation with pilot reuse and IQI were implemented for the proposed channel in [12]. Also, in [13], the achievable SE expressions for CF mMIMO systems with IQI and multi-antenna UEs were derived. However, these works neglected the fact that the IQI and quantization distortion exist in the system simultaneously and those results, e.g., [11]–[13], failed in characterizing the actual system performance.

Motivated by the aforementioned observations, in this paper, we investigate the UL SE performance of CF mMIMO systems with both the low-resolution ADCs and IQI over spatially correlated Rayleigh fading channels. Firstly, we derive novel and exact closed-form uplink SE expressions of the considered system. Secondly, we reveal the impacts of different combining schemes, numbers of quantization bits,

$$\mathbf{R}_{mk} = \left(\mathbf{U}_{mk,t}^* \otimes \mathbf{U}_{mk,r}\right) \mathrm{diag}\left(\mathrm{vec}\left(\mathbf{W}_{mk}\right)\right)\left(\mathbf{U}_{mk,t}^* \otimes \mathbf{U}_{mk,r}\right)^H$$

$$= \sum_{l=1}^{L}\sum_{n=1}^{N}[\mathbf{W}_{mk}]_{ln}\left(\mathbf{u}_{mk,t,n}^* \otimes \mathbf{u}_{mk,r,l}\right)\left(\mathbf{u}_{mk,t,n}^* \otimes \mathbf{u}_{mk,r,l}\right)^H. \tag{2}$$

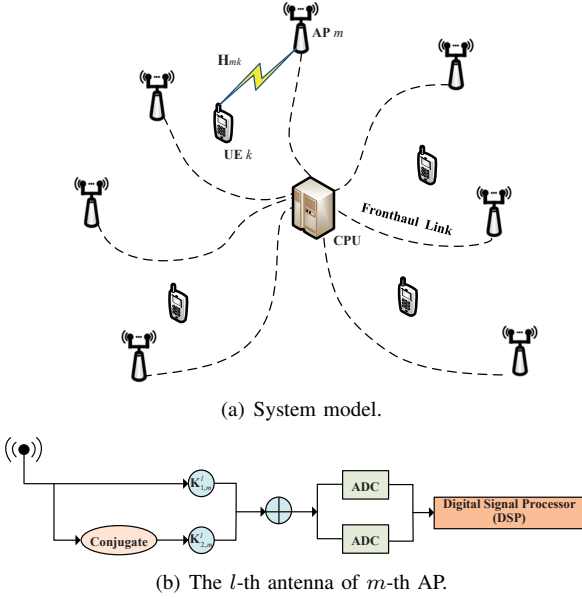(a) System model.

(b) The l-th antenna of m-th AP.

Fig. 1. UL CF mMIMO system with IQI and low-resolution ADCs.

and IQI parameters on the UL SE performance. Our analysis unveils that hardware impairments have significant impacts on the performance of CF mMIMO systems. However, for L-MMSE combining, we can increase the number of APs to compensate the performance degradation caused by hardware impairments.

Notations: The boldface lowercase letters $\mathbf{x}$ and boldface uppercase letters $\mathbf{X}$ denote the column vectors and matrices, respectively. The subscripts $(\cdot)^*$, $(\cdot)^T$, and $(\cdot)^H$ represent conjugate, transpose, and conjugate transpose, respectively. $\mathbb{E}\{\cdot\}$, $\mathrm{tr}\{\cdot\}$ and $\triangleq$ respresent the expectation operator, the trace operator and the definitions, respectively. $\mathrm{vec}(\mathbf{A})$ is the result of stacking the columns of $\mathbf{A}$ on the first column vector in order. $\otimes$ and $\odot$ denote the Kronecker products and the element-wise products, respectively. $\mathbf{x} \sim \mathcal{N}_{\mathbb{C}}\left(\mathbf{0}, \mathbf{R}\right)$ represents a circularly symmetric complex Gaussian distribution vector with zero mean and the covariance $\mathbf{R}$.

II. SYSTEM MODEL

In this paper, we consider a CF mMIMO system operating in the time division duplex (TDD) mode as Fig. 1, where M APs and K UEs are arbitrarily located within a wide service area. Each AP has L antennas and each UE has N antennas. All the APs connect to a central processing unit (CPU) via lossless fronthaul links [4]–[6]. There are two low-resolution ADCs at each antenna of per AP for quantizing signals. Let $\mathbf{H}_{mk} \in \mathbb{C}^{L \times N}$ denote the channel response between the L antennas of AP m and the N antennas of UE k. The channel

responses $\mathbf{H}_{mk}$ remain constant over a coherence time block of τ_c channel uses, which consists of τ_p that is reserved for pilots training and the remaining $\tau_u = \tau_c - \tau_p$ reserved for payload data.

A. Weichselberger Rayleigh Fading Channels

We consider the Weichselberger Rayleigh fading channels shown in [4] as

$$\mathbf{H}_{mk} = \mathbf{U}_{mk,r}(\tilde{\mathbf{W}}_{mk} \odot \mathbf{H}_{mk,iid})\mathbf{U}_{mk,t}^H, \tag{1}$$

where $\mathbf{H}_{mk,iid}$ is an independent and identically distributed (i.i.d.) complex Gaussian random matrix with independent entries satisfying $\mathcal{N}_{\mathbb{C}}\left(0,1\right)$. $\mathbf{U}_{mk,t} = [\mathbf{u}_{mk,t,1}, \cdots, \mathbf{u}_{mk,t,N}] \in \mathbb{C}^{N \times N}$ and $\mathbf{U}_{mk,r} = [\mathbf{u}_{mk,r,1}, \cdots, \mathbf{u}_{mk,r,L}] \in \mathbb{C}^{L \times L}$ denote the eigenvector matrix, respectively, which are obtained by decomposing the one-side correlation matrix $\mathbf{R}_{mk,t} \triangleq \mathbb{E}\left[\mathbf{H}_{mk}^T\mathbf{H}_{mk}^*\right] \in \mathbb{C}^{N \times N}$ at UE k-side and $\mathbf{R}_{mk,r} \triangleq \mathbb{E}\left[\mathbf{H}_{mk}\mathbf{H}_{mk}^H\right] \in \mathbb{C}^{L \times L}$ at AP m-side. The spatial coupling matrix $\mathbf{W}_{mk} \triangleq \tilde{\mathbf{W}}_{mk} \odot \tilde{\mathbf{W}}_{mk} \in \mathbb{R}^{L \times N}$ can fully capture the correlation between AP m and UE k. In addition, $\mathbf{H}_{mk}$ can be represented as $\mathbf{H}_{mk} = [\mathbf{h}_{mk,1}, \cdots, \mathbf{h}_{mk,N}]$, where $\mathbf{h}_{mk,n} \in \mathbb{C}^L$ is the channel between AP m and the n-th antenna of UE k. By applying the vectorization operation for $\mathbf{H}_{mk}$, we can rewrite $\mathbf{h}_{mk} = \mathrm{vec}(\mathbf{H}_{mk}) \sim \mathcal{N}_{\mathbb{C}}\left(\mathbf{0}, \mathbf{R}_{mk}\right)$, where $\mathbf{R}_{mk} \triangleq \mathbb{E}\{\mathrm{vec}\left(\mathbf{H}_{mk}\right)\mathrm{vec}(\mathbf{H}_{mk})^H\} \in \mathbb{C}^{LN \times LN}$ is the positive semidefinite full correlation matrix, which can be expressed as (2) at the top of this page.

On the other hand, the large-scale fading coefficient between AP m and UE k, $\beta_{mk} = \frac{\mathrm{tr}(\mathbf{R}_{mk})}{LN} = \frac{\|\tilde{\mathbf{W}}_{mk}\|_1}{LN}$, describes the geometric pathloss and shadowing. With the block matrix form, we can reconstruct the full correlation matrix $\mathbf{R}_{mk}$, where the (n,i)-th submatrix is $\mathbf{R}_{mk}^{ni} = \mathbb{E}\{\mathbf{h}_{mk,n}\mathbf{h}_{mk,i}^H\}$, where $\mathbf{h}_{mk,n}$ and $\mathbf{h}_{mk,i}$ are the n-th column and i-th column of $\mathbf{H}_{mk}$, respectively.

B. Channel Estimation

In this phase, the channel state information (CSI) are gathered at the APs. Each AP can only exploit its local CSI for receive signals combining [6]. We assume that τ_p mutually orthogonal τ_p-length pilot sequences are used for channel estimation and $\boldsymbol{\Phi}_k \in \mathbb{C}^{\tau_p \times N}$ is the pilot matrix of UE k. If $k = l$, $\boldsymbol{\Phi}_k^H\boldsymbol{\Phi}_l = \boldsymbol{\Phi}_k^T\boldsymbol{\Phi}_l = \tau_p\mathbf{I}_N$ and $\boldsymbol{\Phi}_k^H\boldsymbol{\Phi}_l = \boldsymbol{\Phi}_k^T\boldsymbol{\Phi}_l = \mathbf{0}$ else. We assume $\tau_p \leqslant KN$ such that more than one UE adopt the same pilot matrix. We define that $\mathcal{P}_k$ is the set of UEs that use the same pilot matrix as UE k.

When all the UEs send their respective pilot matrices, the received pilot signal $\mathbf{Y}_m^p \in \mathbb{C}^{L \times \tau_p}$ at the m-th AP is given by $\mathbf{Y}_m^p = \sum_{k=1}^{K}\mathbf{H}_{mk}\boldsymbol{\Omega}_k\boldsymbol{\Phi}_k^T + \mathbf{N}_m^p$, where $\boldsymbol{\Omega}_k \in \mathbb{C}^{N \times N}$ is the UL precoding matrix for UE k during the phase of pilot transmission. Also, we assume that $\boldsymbol{\Omega}_k$ is available at

$$\mathbf{R}_{\widetilde{\mathbf{n}}_{\mathbf{y},m}} = \alpha\left(1-\alpha\right)\mathrm{diag}\left(\sum_{i=1}^{K}\mathbf{\Xi}_{1,m}\mathbf{H}_{mk}\bar{\mathbf{P}}_{k}\mathbf{H}_{mk}^{H}\mathbf{\Xi}_{1,m}^{H} + \sum_{i=1}^{K}\mathbf{\Xi}_{2,m}\mathbf{H}_{mk}^{*}\bar{\mathbf{P}}_{k}^{*}\mathbf{H}_{mk}^{T}\mathbf{\Xi}_{2,m}^{H} + \boldsymbol{\xi}^{2}\right). \tag{4}$$

all the APs and the CPU. $\mathbf{N}_{m}^{p} \in \mathbb{C}^{L \times \tau_{p}}$ is the additive noise at AP m with $\mathcal{N}_{\mathbb{C}}\left(0, \sigma^{2}\right)$ elements, where σ^{2} denotes the noise power. Additionally, the transmission power adopted for channel estimation should be smaller than the maximum transmit power budget $\hat{p}_{k}$ of UE k as $\mathrm{tr}\left(\mathbf{\Omega}_{k}\mathbf{\Omega}_{k}^{H}\right) \leq \hat{p}_{k}$.

We consider the IQI at the AP-side based on the asymmetrical IQI model [11]–[13]. The received pilot signal at AP m can be expressed as $\mathbf{Y}_{iqi,m}^{p} = \mathbf{K}_{1,m}\mathbf{Y}_{m}^{p} + \mathbf{K}_{2,m}(\mathbf{Y}_{m}^{p})^{*} = \sum_{k=1}^{K}\mathbf{K}_{1,m}\mathbf{H}_{mk}\mathbf{\Omega}_{k}\mathbf{\Phi}_{k}^{T} + \sum_{k=1}^{K}\mathbf{K}_{2,m}\mathbf{H}_{mk}^{*}\mathbf{\Omega}_{k}^{*}\mathbf{\Phi}_{k}^{H} + \mathbf{N}_{iqi,m}^{p}$, where $\mathbf{N}_{iqi,m}^{p} = \mathbf{K}_{1,m}\mathbf{N}_{m}^{p} + \mathbf{K}_{2,m}(\mathbf{N}_{m}^{p})^{*} \in \mathbb{C}^{L \times \tau_{p}} \sim \mathcal{N}_{\mathbb{C}}(\mathbf{0}, \lambda^{2}\mathbf{I}_{L})$, and $\lambda^{2} = \sigma^{2}(|\mathbf{K}_{1,m}|^{2} + |\mathbf{K}_{2,m}|^{2})$. Moreover, the received IQI coefficients for AP m are denoted by two $L \times L$ diagonal matrices $\mathbf{K}_{1,m}$ and $\mathbf{K}_{2,m}$, where the diagonal entries $K_{1,m}^{l} = \frac{1}{2}(1 + g_{l}e^{-j\theta_{l}})$ and $K_{2,m}^{l} = \frac{1}{2}(1 - g_{l}e^{j\theta_{l}})$ are the IQI coefficients for the l-th antenna of the m-th AP, with g_{l} and θ_{l} being the amplitude and phase imbalances, respectively. We assume that g_{l} follows the uniform distribution with $\mathcal{U}(1 - g_{l,\max}, 1 + g_{l,\max})$ and θ_{l} has the uniform distribution with $\mathcal{U}(-\theta, \theta)$. We assume that $\mathbf{K}_{1,m}$ and $\mathbf{K}_{2,m}$ are available at all the involved APs.

Moreover, the low-resolution ADCs are implemented to reduce the hardware cost and power consumption. We assume that all the ADCs adopt the same quantization bits and implement the AQNM model to characterize the signal quantization process of the low-resolution ADCs. The received pilot signal with the consideration of low-resolution ADCs is given by $\breve{\mathbf{Y}}_{m}^{p} = \alpha\mathbf{Y}_{iqi,m}^{p} + \breve{\mathbf{N}}_{mq}^{p} = \alpha\sum_{k=1}^{K}\mathbf{K}_{1,m}\mathbf{H}_{mk}\mathbf{\Omega}_{k}\mathbf{\Phi}_{k}^{T} + \alpha\sum_{k=1}^{K}\mathbf{K}_{2,m}\mathbf{H}_{mk}^{*}\mathbf{\Omega}_{k}^{*}\mathbf{\Phi}_{k}^{H} + \alpha\mathbf{N}_{iqi,m}^{p} + \breve{\mathbf{N}}_{mq}^{p}$, where $\breve{\mathbf{N}}_{mq}^{p}$ is the additive Gaussian quantization noise which is uncorrelated with $\mathbf{Y}_{iqi,m}^{p}$. Moreover, α is the linear gain and b_{m} is the number of quantization bits of the low-resolution ADCs.

In order to estimate the channel, the AP projects the quantized signal $\breve{\mathbf{Y}}_{m}^{p}$ onto $\mathbf{\Phi}_{k}^{*}$ as $\mathbf{Y}_{mk}^{p} = \breve{\mathbf{Y}}_{m}^{p}\mathbf{\Phi}_{k}^{*} = \alpha\tau_{p}\sum_{l\in\mathcal{P}_{k}}\mathbf{K}_{1,m}\mathbf{H}_{ml}\mathbf{\Omega}_{l} + \alpha\tau_{p}\sum_{l\in\mathcal{P}_{k}}\mathbf{K}_{2,m}\mathbf{H}_{ml}^{*}\mathbf{\Omega}_{l}^{*} + \mathbf{Q}_{m}^{p} + \mathbf{Q}_{mq}^{p}$, where $\mathbf{Q}_{m}^{p} = \alpha\mathbf{N}_{iqi,m}^{p}\mathbf{\Phi}_{k}^{*} \in \mathbb{C}^{L \times N}$, $\mathbf{Q}_{mq}^{p} = \breve{\mathbf{N}}_{mq}^{p}\mathbf{\Phi}_{k}^{*} \in \mathbb{C}^{L \times N}$. We have $\mathbf{y}_{mk}^{p} = \mathrm{vec}(\mathbf{Y}_{mk}^{p}) \in \mathbb{C}^{LN} = \sum_{l\in\mathcal{P}_{k}}\alpha\tau_{p}\tilde{\mathbf{\Omega}}_{1l}\mathbf{h}_{ml} + \sum_{l\in\mathcal{P}_{k}}\alpha\tau_{p}\tilde{\mathbf{\Omega}}_{2l}\mathbf{h}_{ml}^{*} + \mathbf{q}_{m}^{p} + \mathbf{q}_{mq}^{p}$, where $\tilde{\mathbf{\Omega}}_{1l} = \mathbf{\Omega}_{l}^{T} \otimes \mathbf{K}_{1,m}$, $\tilde{\mathbf{\Omega}}_{2l} = \mathbf{\Omega}_{l}^{H} \otimes \mathbf{K}_{2,m}$, $\mathbf{q}_{m}^{p} = \mathrm{vec}(\mathbf{Q}_{m}^{p}) = \alpha(\mathbf{\Phi}_{k}^{*} \otimes \mathbf{K}_{1,m})\mathrm{vec}(\mathbf{N}_{m}^{p}) + \alpha(\mathbf{\Phi}_{k}^{H} \otimes \mathbf{K}_{2,m})\mathrm{vec}(\mathbf{N}_{m}^{p})^{*}$ and $\mathbf{q}_{mq}^{p} = \mathrm{vec}(\mathbf{Q}_{mq}^{p}) = (\mathbf{\Phi}_{k}^{H} \otimes \mathbf{I}_{L})\mathrm{vec}(\breve{\mathbf{N}}_{mq}^{p})$, respectively.

To derive the upper bound of the system performance[1], we derive the MMSE estimate of $\mathbf{h}_{mk}$ as $\hat{\mathbf{h}}_{mk} = \mathrm{vec}(\hat{\mathbf{H}}_{mk}) = \alpha\mathbf{R}_{mk}\tilde{\mathbf{\Omega}}_{1k}^{H}\mathbf{\Psi}_{mk}^{-1}\mathbf{y}_{mk}^{p}$, where $\mathbf{\Psi}_{mk} = \mathbb{E}\{\mathbf{y}_{mk}^{p}(\mathbf{y}_{mk}^{p})^{H}\}/\tau_{p} = \sum_{l\in\mathcal{P}_{k}}\alpha^{2}\tau_{p}\tilde{\mathbf{\Omega}}_{1l}\mathbf{R}_{ml}\tilde{\mathbf{\Omega}}_{1l}^{H} + \sum_{l\in\mathcal{P}_{k}}\alpha^{2}\tau_{p}\tilde{\mathbf{\Omega}}_{2l}\mathbf{R}_{ml}^{*}\tilde{\mathbf{\Omega}}_{2l}^{H} + \alpha^{2}\lambda^{2}\mathbf{I}_{LN} + \mathbf{R}_{\mathbf{q}_{mq}^{p}}$. The channel

estimate $\hat{\mathbf{h}}_{mk}$ and the channel estimation error $\tilde{\mathbf{h}}_{mk} = \mathrm{vec}(\tilde{\mathbf{H}}_{mk}) = \mathbf{h}_{mk} - \hat{\mathbf{h}}_{mk}$ have the distribution as $\hat{\mathbf{h}}_{mk} \sim \mathcal{N}_{\mathbb{C}}(\mathbf{0}, \hat{\mathbf{R}}_{mk})$, $\tilde{\mathbf{h}}_{mk} \sim \mathcal{N}_{\mathbb{C}}(\mathbf{0}, \mathbf{R}_{mk} - \hat{\mathbf{R}}_{mk})$, where $\hat{\mathbf{R}}_{mk} \triangleq \tau_{p}\alpha^{2}\mathbf{R}_{mk}\tilde{\mathbf{\Omega}}_{1k}^{H}\mathbf{\Psi}_{mk}^{-1}\tilde{\mathbf{\Omega}}_{1k}\mathbf{R}_{mk}$. Besides, $\mathbf{R}_{mk}$ can also be expressed into a block matrix form, where the (n,i)-th submatrix is $\hat{\mathbf{R}}_{mk}^{ni} = \mathbb{E}\{\hat{\mathbf{h}}_{mk,n}\hat{\mathbf{h}}_{nk,i}^{H}\}$. $\hat{\mathbf{h}}_{mk,n}$ and $\hat{\mathbf{h}}_{mk,i}$ are the n-th column and the i-th column of $\hat{\mathbf{H}}_{mk}$, respectively.

C. Data Transmission

During the data transmission phase, all the UEs send information-bearing signals to the APs simultaneously. The signal transmitted by UE k is $\mathbf{s}_{k} = [s_{k,1}, \cdots s_{k,N}]^{T} \in \mathbb{C}^{N}$, which can be denoted as $\mathbf{s}_{k} = \mathbf{P}_{k}\mathbf{x}_{k}$ with $\mathbf{x}_{k} \sim \mathcal{N}_{\mathbb{C}}(0, \mathbf{I}_{N})$ being the data symbol transmitted from UE k. We assume that the precoding matrix $\mathbf{P}_{k} \in \mathbb{C}^{N \times N}$ is available at all the APs and the CPU. Furthermore, the transmitted power should below the maximum transmission power p_{k} of UE k as $\mathrm{tr}\left(\mathbf{P}_{k}\mathbf{P}_{k}^{H}\right) \leq p_{k}, \forall k$.

The received signal, for the case without IQI and low-resolution ADC, $\mathbf{y}_{m} \in \mathbb{C}^{L}$ at AP m is $\mathbf{y}_{m} = \sum_{k=1}^{K}\mathbf{H}_{mk}\mathbf{s}_{k} + \mathbf{n} = \sum_{k=1}^{K}\mathbf{H}_{mk}\mathbf{P}_{k}\mathbf{x}_{k} + \mathbf{n}$, where $\mathbf{n} \sim \mathcal{N}_{\mathbb{C}}\left(\mathbf{0}, \sigma^{2}\mathbf{I}_{L}\right)$ is the independent Gaussian noise. With the consideration of IQI, the received signal at AP m is $\mathbf{y}_{iqi,m} = \sum_{k=1}^{K}\mathbf{\Xi}_{1,m}\mathbf{H}_{mk}\mathbf{P}_{k}\mathbf{x}_{k} + \sum_{k=1}^{K}\mathbf{\Xi}_{2,m}\mathbf{H}_{mk}^{*}\mathbf{P}_{k}^{*}\mathbf{x}_{k}^{*} + \mathbf{n}_{iqi,m}$, where $\mathbf{n}_{iqi,m} = \mathbf{\Xi}_{1,m}\mathbf{n} + \mathbf{\Xi}_{2,m}\mathbf{n}^{*}$, $\mathbf{n}_{iqi,m} \sim \mathcal{N}_{\mathbb{C}}\left(0, \boldsymbol{\xi}^{2}\right)$ and $\boldsymbol{\xi}^{2} = \sigma^{2}(|\mathbf{\Xi}_{1,m}|^{2} + |\mathbf{\Xi}_{2,m}|^{2})\mathbf{I}_{L}$, respectively.

Furthermore, for the case with the quantized signal with the implementation of low-resolution ADCs can be expressed as

$$\breve{\mathbf{y}}_{m} = \alpha\sum_{k=1}^{K}\mathbf{\Xi}_{1,m}\mathbf{H}_{mk}\mathbf{P}_{k}\mathbf{x}_{k} + \alpha\sum_{k=1}^{K}\mathbf{\Xi}_{2,m}\mathbf{H}_{mk}^{*}\mathbf{P}_{k}^{*}\mathbf{x}_{k}^{*}$$
$$+ \alpha\mathbf{n}_{iqi,m} + \breve{\mathbf{n}}_{\mathbf{y},m}, \tag{3}$$

where $\breve{\mathbf{n}}_{\mathbf{y},m}$ is the Gaussian quantization noise, whose covariance matrix $\mathbf{R}_{\breve{\mathbf{n}}_{\mathbf{y},m}} = \alpha(1-\alpha)\mathrm{diag}(\mathbb{E}\{\mathbf{y}_{iqi,m}(\mathbf{y}_{iqi,m})^{H}\})$ is shown in (4) at the top of this page, where $\bar{\mathbf{P}}_{k} = \mathbf{P}_{k}\mathbf{P}_{k}^{H}$.

III. SPECTRAL EFFICIENCY ANALYSIS

Note that the large-scale fading decoding (LSFD) scheme [6], [7] is a promising processing scheme in CF mMIMO systems, which can make the full use of the CF mMIMO topology and achieve excellent performance. We consider a two-layer decoding architecture. Let $\mathbf{V}_{mk} \in \mathbb{C}^{L \times N}$ denote the local combining matrix at AP m designed for UE k. In the first layer, the local estimate of $\mathbf{x}_{k}$ at AP m is

$$\tilde{\mathbf{x}}_{mk} = \mathbf{V}_{mk}^{H}\breve{\mathbf{y}}_{m} = \alpha\sum_{l=1}^{K}\mathbf{V}_{mk}^{H}\mathbf{\Xi}_{1,m}\mathbf{H}_{ml}\mathbf{P}_{l}\mathbf{x}_{l}$$

$$+ \alpha\sum_{l=1}^{K}\mathbf{V}_{mk}^{H}\mathbf{\Xi}_{2,m}\mathbf{H}_{ml}^{*}\mathbf{P}_{l}^{*}\mathbf{x}_{l}^{*} + \alpha\mathbf{V}_{mk}^{H}\mathbf{n}_{iqi,m} + \mathbf{V}_{mk}^{H}\breve{\mathbf{n}}_{\mathbf{y},m}. \tag{5}$$

---

[1]Since the distortion noises caused by hardware impairments depend on the unknown stochastic channel, so there is a correlation between $\hat{\mathbf{h}}_{mk}$ and $\mathbf{h}_{mk}$. However, in order to analyze the upper bound of the system performance, we assume that $\hat{\mathbf{h}}_{mk}$ and $\tilde{\mathbf{h}}_{mk}$ are independent.

$$\mathbf{V}_{mk} = \left(\alpha^2 \sum_{l=1}^{K} \left(\mathbf{\Xi}_{1,m} \hat{\mathbf{H}}_{ml} \bar{\mathbf{P}}_l \hat{\mathbf{H}}_{ml}^H \mathbf{\Xi}_{1,m}^H + \mathbf{\Xi}_{2,m} \hat{\mathbf{H}}_{ml}^* \bar{\mathbf{P}}_l \hat{\mathbf{H}}_{ml}^T \mathbf{\Xi}_{2,m}^H + \tilde{\mathbf{C}}_{ml}^* + \mathbf{C}_{ml}^* \right) + \alpha^2 \boldsymbol{\xi}^2 + \mathbf{R}_{\breve{\mathbf{n}}_{\mathbf{y},m}} \right)^{-1} \hat{\mathbf{H}}_{mk} \mathbf{P}_k. \quad (6)$$

$$\mathbf{\Sigma}_k = \alpha^2 \sum_{l=1}^{K} \mathbf{A}_k^H \mathbb{E} \left\{ \mathbf{G}_{kl,1} \bar{\mathbf{P}}_l \mathbf{G}_{kl,1}^H \right\} \mathbf{A}_k - \mathbf{D}_k \mathbf{D}_k^H + \alpha^2 \sum_{l=1}^{K} \mathbf{A}_k^H \mathbb{E} \left\{ \mathbf{G}_{kl,2} \bar{\mathbf{P}}_l^* \mathbf{G}_{kl,2}^H \right\} \mathbf{A}_k + \alpha^2 \mathbf{A}_k^H \mathbf{F}_{k,1} \mathbf{A}_k + \mathbf{A}_k^H \mathbf{F}_{k,2} \mathbf{A}_k. \quad (10)$$

$$\mathrm{SE}_{k,\max} = \left(1 - \frac{\tau_p}{\tau_c} \right) \log_2 \left| \mathbf{I}_N + \alpha^2 \mathbf{P}_k^H \mathbb{E} \left\{ \mathbf{G}_{kk,1}^H \right\} \left\{ \left(\begin{array}{c} \alpha^2 \sum_{l=1}^{K} \mathbb{E} \left\{ \mathbf{G}_{kl,1} \bar{\mathbf{P}}_l \mathbf{G}_{kl,1}^H \right\} \\ -\alpha^2 \mathbb{E} \left\{ \mathbf{G}_{kk,1} \right\} \bar{\mathbf{P}}_k \mathbb{E} \left\{ \mathbf{G}_{kk,1}^H \right\} \\ +\alpha^2 \sum_{l=1}^{K} \mathbb{E} \left\{ \mathbf{G}_{kl,2} \bar{\mathbf{P}}_l^* \mathbf{G}_{kl,2}^H \right\} + \alpha^2 \mathbf{F}_{k,1} + \mathbf{F}_{k,2} \end{array} \right)^{-1} \mathbb{E} \left\{ \mathbf{G}_{kk,1} \right\} \mathbf{P}_k \right\} \right|. \quad (12)$$

Note that arbitrary combining matrix $\mathbf{V}_{mk}$ holds for (5). Popular linear combining choices are MR combining $\mathbf{V}_{mk} = \hat{\mathbf{H}}_{mk}$ and L-MMSE combining as (6) at the top of this page which can minimize $\mathrm{MSE}_{mk} = \mathbb{E}\{\|\mathbf{x}_k - \mathbf{V}_{mk}^H \breve{\mathbf{y}}_m\|^2 |\hat{\mathbf{H}}_{mk}\}$ with $\tilde{\mathbf{C}}_{ml}^* = \mathbb{E}\{\mathbf{\Xi}_{m,1} \tilde{\mathbf{H}}_{ml} \bar{\mathbf{P}}_l \tilde{\mathbf{H}}_{ml}^H \mathbf{\Xi}_{m,1}^*\}$ and $\mathbf{C}_{ml}^* = \mathbb{E}\{\mathbf{\Xi}_{m,2} \tilde{\mathbf{H}}_l^* \bar{\mathbf{P}}_l^* \tilde{\mathbf{H}}_l^T \mathbf{\Xi}_{m,2}^*\}$.

The second layer of decoding scheme is implemented in the CPU. The local estimates $\tilde{\mathbf{x}}_{mk}$ are sent to the CPU, where $\tilde{\mathbf{x}}_{mk}$ are weighted by LSFD coefficient matrix. Then, we obtain the final decoding signal $\hat{\mathbf{x}}_k = \sum_{m=1}^{M} \mathbf{A}_{mk}^H \tilde{\mathbf{x}}_{mk}$ as

$$\hat{\mathbf{x}}_k = \alpha \sum_{m=1}^{M} \sum_{l=1}^{K} \mathbf{A}_{mk}^H \mathbf{V}_{mk}^H \mathbf{\Xi}_{1,m} \mathbf{H}_{ml} \mathbf{P}_l \mathbf{x}_l \\ + \alpha \sum_{m=1}^{M} \sum_{l=1}^{K} \mathbf{A}_{mk}^H \mathbf{V}_{mk}^H \mathbf{\Xi}_{2,m} \mathbf{H}_{ml}^* \mathbf{P}_l^* \mathbf{x}_l^* + \mathbf{n}_{k1} + \mathbf{n}_{k2}, \quad (7)$$

where the IQI noise term $\mathbf{n}_{k1} = \alpha \sum_{m=1}^{M} \mathbf{A}_{mk}^H \mathbf{V}_{mk}^H \mathbf{n}_{iqi,m}$ and the quantization noise term $\mathbf{n}_{k2} = \sum_{m=1}^{M} \mathbf{A}_{mk}^H \mathbf{V}_{mk}^H \breve{\mathbf{n}}_{\mathbf{y},m}$. We define $\mathbf{A}_k = [\mathbf{A}_{1k}^T, \cdots, \mathbf{A}_{Mk}^T]^T \in \mathbb{C}^{MN \times N}$, $\mathbf{G}_{kl,1} = [\mathbf{V}_{1k}^H \mathbf{\Xi}_{1,1} \mathbf{H}_{1l}, \cdots, \mathbf{V}_{Mk}^H \mathbf{\Xi}_{1,M} \mathbf{H}_{Ml}] \in \mathbb{C}^{MN \times N}$ and $\mathbf{G}_{kl,2} = [\mathbf{V}_{1k}^H \mathbf{\Xi}_{2,1} \mathbf{H}_{1l}^*, \cdots, \mathbf{V}_{Mk}^H \mathbf{\Xi}_{2,M} \mathbf{H}_{Ml}^*] \in \mathbb{C}^{MN \times N}$, respectively. So, (7) can be expressed as

$$\hat{\mathbf{x}}_k = \alpha \mathbf{A}_k^H \mathbf{G}_{kk,1} \mathbf{P}_k \mathbf{x}_k + \alpha \sum_{l=1, l \neq k}^{K} \mathbf{A}_k^H \mathbf{G}_{kl,1} \mathbf{P}_l \mathbf{x}_l \\ + \alpha \sum_{l=1}^{K} \mathbf{A}_k^H \mathbf{G}_{kl,2} \mathbf{P}_l^* \mathbf{x}_l^* + \mathbf{n}_{k1} + \mathbf{n}_{k2}, \quad (8)$$

Since the CPU does not have the knowledge of the channel estimates and only the channel statistics are available, then the classic use-and-then-forget (UatF) bound is applied to calculate the available SE for UE k [6], [4].

Proposition 1. *The achievable SE for UE k is*

$$\mathrm{SE}_k = \left(1 - \frac{\tau_p}{\tau_c} \right) \log_2 \left| \mathbf{I}_N + \mathbf{D}_k^H \mathbf{\Sigma}_k^{-1} \mathbf{D}_k \right|, \quad (9)$$

where $\mathbf{D}_k = \alpha \mathbf{A}_k^H \mathbb{E}\{\mathbf{G}_{kk,1}\} \mathbf{P}_k$. $\mathbf{\Sigma}_k$ is shown in (10), where $\mathbf{F}_{k,1}$ and $\mathbf{F}_{k,2}$ are $M \times M$ diagonal matrix, with the m-th diagonal entries being $\mathbb{E}\{\mathbf{V}_{mk}^H \mathbf{n}_{iqi,m} \mathbf{n}_{iqi,m}^H \mathbf{V}_{mk}\}$ and $\mathbb{E}\{\mathbf{V}_{mk}^H \breve{\mathbf{n}}_{\mathbf{y},m} \breve{\mathbf{n}}_{\mathbf{y},m}^H \mathbf{V}_{mk}\}$.

Proof: The proof is similar to the proof of corollary 2 in [4] and is therefore omitted here due to the page limitation. ∎

The LSFD coefficient matrix $\mathbf{A}_k$ can be optimized by the CPU, then the achievable SE for UE k in (14) can be maximized as the following theorem.

Theorem 1. *The achievable SE in (14) is maximized by*

$$\mathbf{A}_k = \left(\begin{array}{c} \alpha^2 \sum_{l=1}^{K} \mathbb{E} \left\{ \mathbf{G}_{kl,1} \bar{\mathbf{P}}_l \mathbf{G}_{kl,1}^H \right\} \\ +\alpha^2 \sum_{l=1}^{K} \mathbb{E} \left\{ \mathbf{G}_{kl,2} \bar{\mathbf{P}}_l^* \mathbf{G}_{kl,2}^H \right\} \\ +\alpha^2 \mathbf{F}_{k,1} + \mathbf{F}_{k,2} \end{array} \right)^{-1} \mathbb{E} \left\{ \mathbf{G}_{kk,1} \right\} \mathbf{P}_k, \quad (11)$$

which leads to the maximum given in (12) at the top of this page.

More importantly, if the MR combining $\mathbf{V}_{mk} = \hat{\mathbf{H}}_{mk}$ is applied in the first layer, we can derive the closed-form SE expression as follows.

Theorem 2. *When $\mathbf{V}_{mk} = \hat{\mathbf{H}}_{mk}$ is applied in the first layer, we can compute the closed-form SE expression for UE k as* $\mathrm{SE}_{k,MR} = (1 - \frac{\tau_p}{\tau_c}) \log_2 |\mathbf{I}_N + \mathbf{D}_k^H \mathbf{\Sigma}_k^{-1} \mathbf{D}_k|$, *where* $\mathbf{D}_k = \alpha \mathbf{A}_k^H \mathbf{Z}_k \mathbf{P}_k \in \mathbb{C}^{N \times N}$ *and* $\mathbf{\Sigma}_k = \alpha^2 \mathbf{A}_k^H (\sum_{l=1}^{K} \mathbf{T}_{k1,(1)} + \sum_{l \in P_k} \mathbf{T}_{k1,(2)}) \mathbf{A}_k - \mathbf{D}_k \mathbf{D}_k^H + \alpha^2 \sum_{l=1}^{K} \mathbf{A}_k^H (\sum_{l \notin P_k} \mathbf{T}_{k1,(3)} + \sum_{l \in P_k} \mathbf{T}_{k1,(4)}) \mathbf{A}_k + \alpha^2 \mathbf{A}_k^H \mathbf{F}_{k,1} \mathbf{A}_k + \mathbf{A}_k^H \mathbf{F}_{k,2} \mathbf{A}_k \in \mathbb{C}^{N \times N}$ *with* $\mathbf{Z}_k = [\mathbf{Z}_{1k}^T, \cdots, \mathbf{Z}_{Mk}^T]^T$. *The (n,n') element of $\mathbf{Z}_{mk}$ can be denoted as* $[\mathbf{Z}_{mk}]_{nn'} = \sum_{l_1=1}^{L} [\mathbf{\Xi}_{1,m}]_{l_1 l_1} [\hat{\mathbf{R}}_{mk}^{l_1 l_1}]_{nn'}$. *Furthermore,* $\mathbf{T}_{kl,(1)} = diag(\mathbf{\Gamma}_{kl,1}^{(1)}, \cdots, \mathbf{\Gamma}_{kl,M}^{(1)}) \in \mathbb{C}^{MN \times MN}$. *If $m = m'$, the (m,m')-th submatrix of $\mathbf{T}_{kl,(2)} \in \mathbb{C}^{MN \times MN}$ is* $\mathbf{\Gamma}_{kl,m}^{(2)} - \mathbf{\Gamma}_{kl,m}^{(1)}$ *and* $\mathbf{\Lambda}_{mkl} \bar{\mathbf{P}}_l \mathbf{\Lambda}_{m'lk}$ *else. The (m,m)-th submatrix of diagonal matrix $\mathbf{T}_{kl,(3)} \in \mathbb{C}^{MN \times MN}$ and*

$$\left[\mathbf{\Gamma}_{kl,m}^{(x)}\right]_{nn'} = \sum_{i=1}^{N}\sum_{i'=1}^{N} [\bar{\mathbf{P}}_l]_{i'i}\left\{\mathrm{tr}\left(\breve{\mathbf{R}}_{ml,(x/2)}^{i'i}\mathbf{F}_{mkl,(1)}^{n'n}\right) + \alpha^2\tau_p^2\sum_{q_1=1}^{N}\sum_{q_2=1}^{N}\left[\mathrm{tr}\left(\tilde{\mathbf{F}}_{mkl,(2)}^{q_1 n}\tilde{\mathbf{R}}_{ml,(x/2)}^{i'q_1}\right)\mathrm{tr}\left(\tilde{\mathbf{F}}_{mkl,(2)}^{n'q_2}\tilde{\mathbf{R}}_{ml,(x/2)}^{q_2 i}\right)\right]\right.$$

$$+\alpha^2\tau_p^2\sum_{q_1=1}^{N}\sum_{q_2=1}^{N}\left[\mathrm{tr}\left(\tilde{\mathbf{F}}_{mkl,(3)}^{q_1 n}\tilde{\mathbf{R}}_{ml,(x/2)}^{i'q_1}\right)\mathrm{tr}\left(\tilde{\mathbf{F}}_{mkl,(3)}^{n'q_2}\tilde{\mathbf{R}}_{ml,(x/2)}^{q_2 i}\right)\right]$$

$$+\alpha^2\tau_p^2\sum_{q_1=1}^{N}\sum_{q_2=1}^{N}\left[\mathrm{tr}\left(\tilde{\mathbf{F}}_{mkl,(2)}^{q_1 n}\tilde{\mathbf{R}}_{ml,(x/2)}^{i'q_2}\tilde{\mathbf{R}}_{ml,(x/2)}^{q_2 i}\tilde{\mathbf{F}}_{mkl,(2)}^{n'q_1}\right) + \mathrm{tr}\left(\tilde{\mathbf{F}}_{mkl,(3)}^{q_1 n}\tilde{\mathbf{R}}_{ml,(x/2)}^{i'q_2}\tilde{\mathbf{R}}_{ml,(x/2)}^{q_2 i}\tilde{\mathbf{F}}_{mkl,(3)}^{n'q_1}\right)\right]\right\}. \tag{13}$$
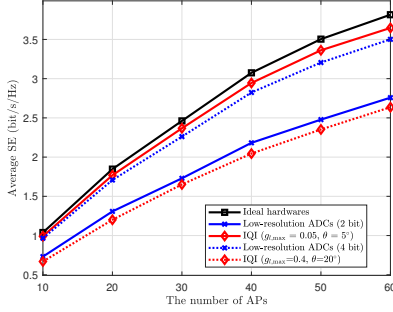

Fig. 2. Average SE versus the number of APs with L-MMSE combining at ideal hardware, low-resolution ADCs ($b = 2/4$), and IQI ($g_{l,\max} = 0.05$, $\theta = 5°$/ $g_{l,\max} = 0.4$, $\theta = 20°$) for $K = 20$, $L = 2$, and $N = 2$.
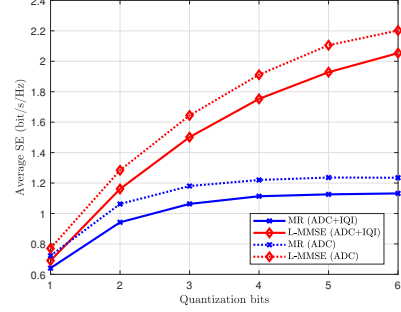

Fig. 3. Average SE against the number of ADC quantization bits with L-MMSE and MR combining for $M = 20$, $K = 20$, $L = 2$, and $N = 2$.

$\mathbf{T}_{kl,(4)} \in \mathbb{C}^{MN \times MN}$ are $\mathbf{\Gamma}_{kl,m}^{(3)}$ and $\mathbf{\Gamma}_{kl,m}^{(4)}$, respectively. The (n, n')-th element of $\mathbf{\Lambda}_{mkl} \in \mathbb{C}^{N \times N}, \mathbf{\Lambda}_{m'lk} \in \mathbb{C}^{N \times N}$ are $[\mathbf{\Lambda}_{mkl}]_{nn'} = \sum_{l_1=1}^{L}[\mathbf{\Xi}_{1,m}]_{l_1 l_1}[\mathbf{\Theta}_{mkl}^{l_1 l_1}]_{nn'}$ and $[\mathbf{\Lambda}_{m'lk}]_{nn'} = \sum_{l_1=1}^{L}[\mathbf{\Xi}_{1,m}]_{l_1 l_1}[\mathbf{\Theta}_{m'lk}^{l_1 l_1}]_{nn'}$, where $\mathbf{\Theta}_{mkl} = \mathbb{E}\{\hat{\mathbf{h}}_{ml}\hat{\mathbf{h}}_{mk}^{H}\} = \tau_p\alpha^2\mathbf{R}_{ml}\tilde{\mathbf{\Omega}}_l^H\mathbf{\Psi}_{mk}^{-1}\tilde{\mathbf{\Omega}}_k\mathbf{R}_{mk}$, $\mathbf{\Theta}_{m'lk} = \mathbb{E}\{\hat{\mathbf{h}}_{m'k}\hat{\mathbf{h}}_{m'l}^{H}\} = \tau_p\alpha^2\mathbf{R}_{m'k}\tilde{\mathbf{\Omega}}_k^H\mathbf{\Psi}_{m'k}^{-1}\tilde{\mathbf{\Omega}}_k\mathbf{R}_{m'l}$. Furthermore, the (n, n')-th element of $\mathbf{\Gamma}_{kl,m}^{(1)} \in \mathbb{C}^{N \times N}, \mathbf{\Gamma}_{kl,m}^{(3)} \in \mathbb{C}^{N \times N}$ are $[\mathbf{\Gamma}_{kl,m}^{(1)}]_{nn'} = \sum_{i=1}^{N}\sum_{i'=1}^{N}[\bar{\mathbf{P}}_l]_{i'i}\mathrm{tr}(\breve{\mathbf{R}}_{ml,(1)}^{i'i}\hat{\mathbf{R}}_{mk}^{n'n})$ and $[\mathbf{\Gamma}_{kl,m}^{(3)}]_{nn'} = \sum_{i=1}^{N}\sum_{i'=1}^{N}[\bar{\mathbf{P}}_l]_{i'i}\mathrm{tr}(\breve{\mathbf{R}}_{ml,(2)}^{i'i}\hat{\mathbf{R}}_{mk}^{n'n})$, respectively. The (n, n')-th element of $\mathbf{\Gamma}_{mkl}^{(x)}$, $\forall x \in \{2, 4\}$, is shown as (13) at the top of this page, where $\tilde{\mathbf{F}}_{mkl,(2)}^{nq}$, $\tilde{\mathbf{F}}_{mkl,(3)}^{nq}$, $\tilde{\mathbf{R}}_{ml,(1)}^{nq}$ and $\tilde{\mathbf{R}}_{ml,(2)}^{nq}$ are the (n, q)-th submatrix of $(\mathbf{F}_{mkl,(2)})^{\frac{1}{2}}$, $(\mathbf{F}_{mkl,(3)})^{\frac{1}{2}}$, $\breve{\mathbf{R}}_{ml,(1)}^{\frac{1}{2}}$ and $\breve{\mathbf{R}}_{ml,(2)}^{\frac{1}{2}}$, respectively.

Proof: The proof is given in the appendix. ∎

Remark 1. *The linear gain α and $\mathbf{F}_{k,2}$ denote the impacts caused by the low-resolution ADCs. $\mathbf{T}_{kl,(1)}$ and $\mathbf{T}_{kl,(2)}$ are the result of decomposing $\mathbb{E}\{\mathbf{G}_{kl,1}\bar{\mathbf{P}}_l\mathbf{G}_{kl,1}^{H}\}$ and the same goes for $\mathbf{T}_{kl,(3)}$, $\mathbf{T}_{kl,(4)}$, which include the impacts of IQI, as well as $\mathbf{F}_{k,1}$. We can observe that the low-resolution ADCs quantify the IQI noise from (3), and the quantization noise is also connected with the result of the IQI from (4).*

IV. NUMERICAL RESULTS

In this section, we investigate the impacts of the low-resolution ADCs and IQI on the CF mMIMO system. We assume the same IQI coefficients at the AP antenna for both the phase of channel estimate and data transmission. Besides,

the IQI paraments g_l, θ_l are distributed as $g_l \sim \mathcal{U}(0.95, 1.05)$ and $\theta_l \sim \mathcal{U}(-5°, 5°)$, unless specified. Additionally, we adopt the same parameters setting as in [4].

In Fig. 2, we investigate the average SE as a function of the number of APs M for different parameters with the L-MMSE combining. We also consider the case with perfect ADCs and without the IQI, which undoubtedly achieves the best SE performance, as a baseline to show the upper bound performance. It can be found that the average SE increases with M since the newly introduced APs offer more spatial degrees-of-freedom to provide high quality service for a fewer number of UEs. Note that both the IQI and low-resolution ADCs reduce the UL SE performance. More importantly, the damage caused by the IQI on the CF mMIMO is more severe than that of the low-resolution ADCs, e.g., the SE performance decreases by 30.91% when the IQI parameters are set with $g_{l,\max} = 0.4$, $\theta = 20°$ compared with the perfect hardwares scenario, for $M = 60$. It can be observed that for L-MMSE combining, increasing the number of APs is an effective way to compensate the low-resolution ADCs and IQI.

In Fig. 3, the average SE achieved with/without IQI is plotted as a function of the quantization bits. It is shown that the average SE increases with b_m but cannot fully compensate the gap between a perfectly IQ matched and an IQI system. When the number of quantization bits is up to 5 bit, the system with the MR combining achieves its upper bound performance and keeps steady in spite of the increase of b_m. However, for the L-MMSE combining, there is still room for improvement in the SE for when $b_m > 6$. As expected, the L-MMSE combining outperforms MR combining since it can
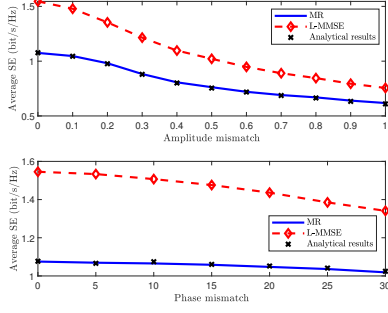
Fig. 4. Average SE against amplitude mismatch and phase mismatch with L-MMSE and MR combining for $M = 20$, $K = 20$, $L = 2$, $N = 2$ and $b_m = 4$.

achieve the best balance between amplifying the desired signal and suppressing the interference. In fact, compared with MR combining, the SE can achieve a dramatic improvement by 81.45% with L-MMSE combining when $b_m = 6$.

In Fig. 4, we focus on the impact of the IQI coefficients on the average SE. When $g_{l,\max} = 0$ and $\theta = 0°$, corresponding to the perfect IQ matching, the average SE reaches the maximum value as 1.56 bit/s/Hz. Furthermore, the amplitude mismatch introduces a severe deterioration on the average SE than that of the phase mismatch. Note that the results of the closed-form SE expressions for the MR combining in Theorem 2 match perfectly the results generated by the Monte-Carlo method, validating the accuracy of the derived closed-form SE expressions.

V. Conclusions

In this paper, we investigated the UL SE performance for a CF mMIMO system with low-resolution ADCs and IQI over Rayleigh correlated channel, where both the APs and UEs are equipped with multiple antennas. We derived the achievable uplink SE expressions with the MR combining and L-MMSE combining taking both the IQI and quantization distortion into account. The numerical results showed that the impacts induced by the low-resolution ADCs and IQI cannot be completely eliminated by increasing the number of APs with the L-MMSE combining. In general, an amplitude mismatch is more harmful than a phase mismatch to the system performance.

VI. Appendix

The term $\mathbf{D}_k = \alpha \mathbf{A}_k^H \mathbb{E}\{\mathbf{G}_{kk,1}\}\mathbf{P}_k$ with $\mathbb{E}\{\mathbf{G}_{kk,1}\} = \left[\mathbb{E}\{\mathbf{V}_{1k}^H \mathbf{\Xi}_{1,1} \mathbf{H}_{1k}\};\cdots;\mathbb{E}\{\mathbf{V}_{Mk}^H \mathbf{\Xi}_{1,M} \mathbf{H}_{Mk}\}\right] = [\mathbf{Z}_{1k};\cdots;\mathbf{Z}_{Mk}]$, where $\mathbf{Z}_{mk} = \mathbb{E}\{\mathbf{V}_{mk}^H \mathbf{\Xi}_{m,1} \mathbf{H}_{mk}\} = \mathbb{E}\{\hat{\mathbf{H}}_{mk}^H \mathbf{\Xi}_{m,1} \hat{\mathbf{H}}_{mk}\}$, and the (n, n')-th element of which is $[\mathbf{Z}_{mk}]_{nn'} = \sum_{l_1=1}^{L}[\mathbf{\Xi}_{m,1}]_{l_1 l_1}[\hat{\mathbf{R}}_{mk}^{l_1 l_1}]_{nn'}$.

The (m, m')-th submatrix of $\mathbb{E}\{\mathbf{G}_{kl,1}\bar{\mathbf{P}}_l \mathbf{G}_{kl,1}^H\} \in \mathbb{C}^{MN \times MN}$ is $\mathbb{E}\{\mathbf{V}_{mk}^H \mathbf{\Xi}_{1,m} \mathbf{H}_{ml}\bar{\mathbf{P}}_l \mathbf{H}_{m'l}^H \mathbf{\Xi}_{1,m'}^* \mathbf{V}_{m'k}\}$. Firstly, we divided the submatrix into four situations as described below. **Case 1** ($m \neq m', l \notin \mathcal{P}_k$) and **case 2** ($m \neq m', l \in \mathcal{P}_k$) are similar with the result in [4]. So, we emphasize on **case 3** ($m = m', l \notin \mathcal{P}_k$). We define the symbol $\langle \mathbf{A}, N \rangle$ which represents repeating the column

vector $\mathbf{A}$ over N rows. In order to simplify the analysis, we assume that the new effective channel is $\breve{\mathbf{H}}_{ml}^{m,1} = \mathbf{\Xi}_{1,m}\mathbf{H}_{ml}$, so the spatial correlation matrix of $\breve{\mathbf{H}}_{ml}^{m,1}$ can be calculated as $\breve{\mathbf{R}}_{ml,(1)} = \mathbb{E}\{\mathrm{vec}(\breve{\mathbf{H}}_{ml}^{m,1})\mathrm{vec}(\breve{\mathbf{H}}_{ml}^{m,1})^H\} = \langle \mathrm{diag}(\mathbf{\Xi}_{1,m}), N \rangle \bullet \langle (\mathrm{diag}(\mathbf{\Xi}_{1,m})), N \rangle^H \odot \mathbf{R}_{ml}$. So, we define $\mathbf{\Gamma}_{mkl}^{(1)} = \mathbb{E}\{\mathbf{V}_{mk}^H \mathbf{\Xi}_{1,m}\mathbf{H}_{ml}\bar{\mathbf{P}}_l \mathbf{H}_{m'l}^H \mathbf{\Xi}_{1,m'}^* \mathbf{V}_{m'k}\} = \mathbb{E}\{\mathbf{V}_{mk}^H \breve{\mathbf{H}}_{ml}^{m,1}\bar{\mathbf{P}}_l (\breve{\mathbf{H}}_{m'l}^{m',1})^H \mathbf{V}_{m'k}\}$ and the (n, n')-th element of which is $[\mathbf{\Gamma}_{mkl}^{(1)}]_{nn'} = \sum_{i=1}^{N}\sum_{i'=1}^{N}[\bar{\mathbf{P}}_l]_{i'i}\mathrm{tr}(\breve{\mathbf{R}}_{ml,(1)}\hat{\mathbf{R}}_{mk}^{n'n})$.

For **case 4**, where $m = m'$ and $l \in \mathcal{P}_k$, we define that $\mathbf{\Gamma}_{mkl}^{(2)} \triangleq \mathbb{E}\{\mathbf{V}_{mk}^H \breve{\mathbf{H}}_{ml}^{m,1}\bar{\mathbf{P}}_l (\breve{\mathbf{H}}_{m'l}^{m',1})^H \mathbf{V}_{m'k}\}$ with the (n, n')-th element being $[\mathbf{\Gamma}_{mkl}^{(2)}]_{nn'} = \sum_{i=1}^{N}\sum_{i'=1}^{N}[\bar{\mathbf{P}}_l]_{i'i}\mathbb{E}\{\hat{\mathbf{h}}_{mk,n}^H \breve{\mathbf{h}}_{ml,i'}^{m,1}(\breve{\mathbf{h}}_{ml,i}^{m,1})^H \hat{\mathbf{h}}_{mk,n'}\}$.
Let $\mathbf{x}_{mk}^p = \mathbf{y}_{mk}^p - \alpha\tau_p\tilde{\mathbf{\Omega}}_{1l}\mathbf{h}_{ml} - \alpha\tau_p\tilde{\mathbf{\Omega}}_{2l}\mathbf{h}_{ml}^*$ and $\mathbf{S}_{mk} = \alpha\mathbf{R}_{mk}\tilde{\mathbf{\Omega}}_{1k}^H\mathbf{\Psi}_{mk}^{-1}$. By decomposing $\mathbb{E}\{|\hat{\mathbf{h}}_{mk}^H \breve{\mathbf{h}}_{ml}|^2\}$, the term $\mathbb{E}\{\hat{\mathbf{h}}_{mk,n}^H \breve{\mathbf{h}}_{ml,i'}^{m,1}(\breve{\mathbf{h}}_{ml,i}^{m,1})^H \hat{\mathbf{h}}_{mk,n'}\}$ equals to $\mathbb{E}\{[\mathbf{S}_{mk}\mathbf{x}_{mk}^p]_n^H \breve{\mathbf{h}}_{ml,i'}^{m,1}(\breve{\mathbf{h}}_{ml,i}^{m,1})^H[\mathbf{S}_{mk}\mathbf{x}_{mk}^p]_{n'}\} + \alpha^2\tau_p^2\mathbb{E}\{[\mathbf{S}_{mk}\tilde{\mathbf{\Omega}}_{1l}\mathbf{h}_{ml}]_n^H \breve{\mathbf{h}}_{ml,i'}^{m,1}(\breve{\mathbf{h}}_{ml,i}^{m,1})^H[\mathbf{S}_{mk}\tilde{\mathbf{\Omega}}_{1l}\mathbf{h}_{ml}]_{n'}\} + \alpha^2\tau_p^2\mathbb{E}\{[\mathbf{S}_{mk}\tilde{\mathbf{\Omega}}_{2l}\mathbf{h}_{ml}^*]_n^H \breve{\mathbf{h}}_{ml,i'}^{m,1}(\breve{\mathbf{h}}_{ml,i}^{m,1})^H[\mathbf{S}_{mk}\tilde{\mathbf{\Omega}}_{2l}\mathbf{h}_{ml}^*]_{n'}\}$, and the remaining steps are similar to [4]. The second part $\mathbb{E}\{\mathbf{G}_{kl,2}\bar{\mathbf{P}}_l^* \mathbf{G}_{kl,2}^H\}$ can also be divided into four cases as $\mathbb{E}\{\mathbf{G}_{kl,1}\bar{\mathbf{P}}_l \mathbf{G}_{kl,1}^H\}$.

References

[1] J. Zhang, E. Björnson, M. Matthaiou, D. W. K. Ng, H. Yang, and D. J. Love, "Prospective multiple antenna technologies for beyond 5G," *IEEE J. Sel. Areas Commun*, vol. 38, no. 8, pp. 1637–1660, Jun. 2020.

[2] H. Q. Ngo, A. Ashikhmin, H. Yang, E. G. Larsson, and T. L. Marzetta, "Cell-free massive MIMO versus small cells," *IEEE Trans. Wireless Commun.*, vol. 16, no. 3, pp. 1834–1850, Mar. 2017.

[3] Y. Xiong, N. Wei, Z. Zhang, B. Li, and Y. Chen, "Channel estimation and IQ imbalance compensation for uplink massive MIMO systems with low-resolution ADCs," *IEEE Access*, vol. 5, pp. 6372–6388, Apr. 2017.

[4] Z. Wang, J. Zhang, B. Ai, C. Yuen, and M. Debbah, "Uplink performance of cell-free massive MIMO with multi-antenna users over jointly-correlated Rayleigh fading channels," *IEEE Trans. Wireless Commun.*, Mar. 2022.

[5] J. Zhang, J. Zhang, D. W. K. Ng, S. Jin, and B. Ai, "Improving sum-rate of cell-free massive MIMO with expanded compute-and-forward," *IEEE Trans. Signal Process.*, vol. 70, pp. 202–215, Nov. 2022.

[6] E. Björnson and L. Sanguinetti, "Making cell-free massive MIMO competitive with MMSE processing and centralized implementation," *IEEE Trans. Wireless Commun.*, vol. 19, no. 1, pp. 77–90, Jan. 2019.

[7] S. Chen, J. Zhang, J. Zhang, E. Björnson, and B. Ai, "A survey on user-centric cell-free massive MIMO systems," *Digit. Commun. Netw.*, Dec. 2021.

[8] J. Zhang, J. Zhang, D. W. K. Ng, S. Jin, and B. Ai, "Improving sum-rate of cell-free massive MIMO with expanded compute-and-forward," *IEEE Trans. Signal Process.*, vol. 70, pp. 202–215, 2021.

[9] Y. Zhang, M. Zhou, X. Qiao, H. Cao, and L. Yang, "On the performance of cell-free massive MIMO with low-resolution ADCs," *IEEE Access*, vol. 7, pp. 117 968–117 977, Aug. 2019.

[10] Y. Zhang, M. Zhou, H. Cao, L. Yang, and H. Zhu, "On the performance of cell-free massive MIMO with mixed-ADC under Rician fading channels," *IEEE Commun. Lett.*, vol. 24, no. 1, pp. 43–47, Jan. 2020.

[11] R. Mahendra, S. K. Mohammed, and R. K. Mallik, "Performance of MRC and ZF receivers in IQ-Impaired uplink massive MIMO systems," pp. 202–206, Feb. 2021.

[12] Y. Chen, L. You, X. Gao, and X.-G. Xia, "Channel estimation with pilot reuse in IQ imbalanced massive MIMO," *IEEE Access*, vol. 8, pp. 1542–1555, Dec. 2019.

[13] J. A. C. Sutton, H. Q. Ngo, and M. Matthaiou, "Cell-free massive MIMO with multiple-antenna users under I/Q imbalance," in *EUSIPCO*, Dec. 2021, pp. 920–924.